Acoustic Determination of Thermophysical Properties and Critical Parameters for R404A and Critical Line of $xCO_2 + (1 - x)$R404A

José M. S. S. Esperança, Pedro F. Pires, Henrique J. R. Guedes, Nuno Ribeiro, Tânia Costa, and Ana Aguiar-Ricardo*

REQUIMTE/CQFB, Departamento de Química, Faculdade de Ciências e Tecnologia, Universidade Nova de Lisboa, 2829-516 Caparica, Portugal

The thermophysical properties and critical parameters for the alternative refrigerant R404A (52 wt % of 1,1,1-trifluoroethane (R143a) + 44 wt % of pentafluoroethane (R125) + 4 wt % of 1,1,1,2-tetrafluoroethane (R134a)) were investigated using two different acoustic techniques. The critical behavior of the system $xCO_2 + (1 - x)$R404A was also investigated. Experimental data of speed of sound in liquid R404A from 258 K to 338 K and pressures up to 65 MPa were measured using a pulse-echo method. Derived thermodynamic properties are calculated, combining our experimental data with density and isobaric heat capacity values published by other authors. Measurements of the critical temperature T_c and pressure p_c on (R404A) and mixtures of $xCO_2 + (1 - x)$R404A were performed using another simple ultrasonic time-delay technique. The binary critical line was determined over the whole composition range showing that this system deviates only slightly from ideality since the critical line is a continuous line. The Peng−Robinson equation of state with conventional mixing and combining rules was used to correlate the binary experimental data.

Introduction

Fluorinated alkanes (HFCs) represent the vast majority of chlorofluorocarbons (CFCs) and hydrochlorofluorocarbons (HCFC) substitutes. The technical challenges of the CFC phase out are mostly overcome, but the HCFC phase-out cannot be regarded as finalized.

R404A is a near azeotropic ternary mixture containing 52 wt % of 1,1,1-trifluoroethane (R143a), 44 wt % of pentafluoroethane (R125), and 4 wt % of 1,1,1,2-tetrafluoroethane (R134a). R404A has been internationally endorsed as the industry-standard, long-term HFC replacement for R-502 refrigerant, an azeotropic blend of HCFC-22 and CFC-115, in commercial refrigeration equipment.[1−3] It was also recognized that this mixture was a good replacement for HCFC-22.[4] Its physical and thermodynamic properties are comparable to those of R-502, and it is nonflammable. Besides several applications, the retrofit of existing R-502 installations with R404A is possible.[5] Its ozone depletion potential is zero and its halocarbon global warming potential is 0.83, much lower when compared to R-502 (19.4). Despite being considered one of the most suitable HFC replacements for R-502, there are very few property measurements reported in the literature.

The speed of sound (u) is a thermodynamic property that can be experimentally determined with great accuracy over a large range of temperature and pressure conditions, in both the liquid and the gas phases. Since u can be related to the first pressure partial derivative of the density, high-accuracy speed of sound data can be used to enhance the development of equations of state. Also, it is very useful as a source of information to compute the values of other thermodynamic properties that are difficult to obtain at extreme experimental conditions, such as calorimetric data at high pressures. In the present work, we have measured the ultrasonic speed of propagation in liquid R-404a with an apparatus designed to operate at high pressures. This apparatus has been tested, and the results are reported for three other alternative refrigerants.[6−9] The experimental data were fitted and used together with density and isobaric heat capacity data from REFPROP[10] to calculate, through an integration method,[11] several thermodynamic properties such as the isentropic and isothermal compressibilities (κ_S and κ_T), the isobaric thermal expansion coefficient (α_p), the thermal pressure coefficient (γ_v), the isenthalpic Joule−Thomson coefficient (μ_{JT}), the isobaric and isochoric heat capacities (C_P and C_V), and the enthalpy and entropy variations relative to a reference state.

Recent works have shown that it seems likely that blends of new refrigerants rather than pure substances will replace the common CFCs. Vapor−liquid equilibrium data are required in order to evaluate the performance of refrigeration cycles. Moreover, apart from other important physicochemical properties, the knowledge of critical parameters is essential to design a simple process. Mixtures of partially fluorinated gases with CO_2 can be used as refrigerants or as modifiers to improve solubility in supercritical fluids. Therefore, knowledge of their phase behavior is crucial. In this work, critical properties of the refrigerant R404A and their mixtures with CO_2 were investigated. To that end, we applied an acoustic simple technique that proved to be a reliable method to explore the critical behavior of multicomponent systems as reported in previous works.[12−17] Measurements of the critical temperature T_c and pressure p_c of the CO_2 + R404A mixtures were performed over the whole composition range. The Peng−Robinson equation of state, with conventional mixing and combining rules, was used to correlate the experimental data.

Experimental Section

Materials. The R404A used in the experimental work was supplied by Solvay Fluor und Derivate GmbH, with a stated composition of 52/44/4 wt % of R143a/R125/R134a, respec-

* To whom correspondence should be addressed. Fax: +351 212948385. Tel: +351 212949648. E-mail: aar@dq.fct.unl.pt.

10.1021/je0600707 CCC: $33.50
Published on Web 04/22/2006

Table 1. Experimental Speed of Sound, u/m·s^{-1}, for Alternative Refrigerant Mixture R404A as a Function of Temperature T and Pressure p

T = 258.13 K		T = 268.12 K		T = 278.10 K		T = 288.18 K		T = 298.17 K		T = 308.17 K		T = 318.16 K		T = 328.18 K		T = 338.19 K	
p	u	p	u	p	u	p	u	p	u	p	u	p	u	p	u	p	u
MPa	m·s^{-1}	MPa	m·s^{-1}	MPa	m·s^{-1}	MPa	m·s^{-1}	MPa	m·s^{-1}	MPa	m·s^{-1}	MPa	m·s^{-1}	MPa	m·s^{-1}	MPa	m·s^{-1}
0.59	579.4	0.52	529.6	0.71	481.9	0.95	433.0	1.26	383.8	1.62	332.9	2.06	279.2	2.59	221.3	3.22	155.0
0.59	579.3	0.62	530.8	0.71	481.8	0.95	433.0	1.26	383.9	1.62	333.0	2.06	279.4	2.59	221.3	3.22	155.1
0.64	579.7	0.71	531.7	0.71	481.9	1.00	433.8	1.30	384.6	1.62	332.9	2.06	279.3	2.65	224.4	3.31	164.1
0.71	580.4	0.75	532.1	0.75	482.2	1.11	435.4	1.41	386.6	1.70	334.6	2.10	280.4	2.75	229.1	3.50	181.4
0.75	580.7	0.80	532.7	0.80	482.9	1.26	437.6	1.50	388.3	1.80	337.1	2.21	283.8	3.01	240.6	3.75	197.3
0.80	581.3	0.90	533.8	0.90	484.2	1.50	441.2	1.75	392.9	1.90	339.4	2.36	288.3	3.25	250.2	4.00	210.6
0.90	582.1	1.00	534.9	1.00	485.5	1.75	444.9	2.01	397.4	2.01	341.8	2.51	292.8	3.50	259.2	4.50	231.1
1.00	583.1	1.26	537.6	1.26	488.8	2.01	448.5	2.25	401.5	2.25	347.2	2.75	299.9	4.00	275.1	5.00	248.4
1.26	585.5	1.26	537.7	1.26	488.9	2.25	452.0	2.51	405.8	2.51	352.6	3.01	306.7	4.50	289.1	6.01	277.1
1.50	588.0	1.50	540.4	1.50	491.8	2.51	455.4	2.75	409.8	2.75	357.7	3.50	319.1	5.00	301.8	7.01	300.5
1.75	590.3	1.75	543.1	1.75	494.8	2.75	458.7	3.01	413.8	3.01	362.8	4.00	330.5	6.01	324.1	8.00	320.9
2.01	592.6	2.01	545.7	2.01	498.0	3.01	462.2	3.50	421.6	3.50	372.3	4.50	341.2	7.01	343.3	9.00	339.0
2.25	594.8	2.25	548.2	2.25	500.8	3.50	468.7	4.00	429.0	4.00	381.3	5.00	350.8	8.00	360.5	10.00	355.3
2.51	597.2	2.51	550.8	2.51	503.9	4.00	475.1	4.50	436.1	4.50	389.7	6.01	369.0	9.00	376.4	12.00	384.4
2.75	599.4	2.75	553.2	2.75	506.8	4.50	481.3	5.00	443.0	5.00	397.8	7.01	385.3	10.00	391.0	14.00	410.0
3.01	601.7	3.01	555.9	3.01	509.6	5.00	487.2	6.01	456.3	6.01	412.9	8.00	400.5	12.00	417.3	16.01	432.8
3.50	606.1	3.50	560.7	3.50	515.4	6.01	498.8	7.01	468.5	7.01	427.2	9.00	414.5	14.00	440.8	18.00	453.8
4.00	610.5	4.00	565.8	4.00	520.8	7.01	509.7	8.00	480.2	8.00	440.2	10.00	427.4	16.01	462.2	20.00	473.0
4.50	614.7	4.50	570.6	4.50	526.2	8.00	520.2	9.00	491.4	9.00	452.6	12.00	451.3	18.00	482.0	23.00	499.9
5.00	619.0	5.00	575.4	5.00	531.6	9.00	530.3	10.00	501.9	10.00	464.4	14.00	473.0	20.00	500.4	26.00	524.3
6.01	627.1	6.01	584.4	6.01	541.8	10.00	539.9	12.00	521.9	12.00	486.1	16.01	493.0	23.00	525.8	29.01	546.9
7.01	635.3	7.01	593.2	7.01	551.6	12.00	558.1	14.00	540.3	14.00	506.1	18.00	511.4	26.00	549.3	32.25	569.6
8.00	643.1	7.01	593.2	8.00	561.0	14.00	575.4	16.01	557.6	16.01	524.7	20.00	528.8	29.01	571.0	35.00	587.4
9.00	650.6	8.00	601.8	9.00	570.1	16.01	591.5	18.00	573.9	18.00	542.2	23.00	552.9	32.25	593.2	40.00	618.0
10.00	658.1	9.00	610.3	10.00	578.9	18.00	606.9	20.00	589.6	20.00	558.6	26.00	575.7	35.00	610.4	45.01	646.5
12.00	672.5	10.00	618.2	12.00	595.7	20.00	621.5	23.00	611.3	23.00	581.6	29.01	596.7	40.00	640.3	50.00	673.1
14.00	686.3	12.00	633.7	14.00	611.7	23.00	642.1	26.00	631.8	26.00	603.0	32.25	617.9	45.01	668.3	55.00	698.2
16.01	699.5	14.00	648.4	16.01	626.7	26.00	661.4	29.01	650.9	29.01	623.1	35.00	634.2	50.00	694.1	59.99	721.6
16.01	699.5	16.01	662.4	18.00	640.9	29.01	679.9	32.25	670.9	32.25	643.9	40.00	663.6	55.00	718.5	65.00	744.4
18.00	711.7	18.00	675.9	20.00	654.7	32.25	699.1	35.00	686.5	35.00	659.9	45.01	690.7	59.99	741.7		
20.00	723.9	20.00	689.0	23.00	674.4	35.00	714.1	40.00	714.0	40.00	688.2	50.00	716.1	65.00	763.6		
23.00	741.6	23.00	707.3	26.00	692.6	40.00	740.3	45.01	739.2	45.01	714.7	55.01	740.1				
26.00	758.3	26.00	725.0	29.01	710.3	45.01	765.3	50.00	763.5	49.99	739.1	60.01	762.8				
29.01	774.3	29.01	741.9	32.31	728.8	50.00	788.3	55.00	786.2	55.01	762.7	65.00	784.4				
32.25	791.1	32.25	759.3	35.00	742.9	55.00	810.4	60.00	807.6	60.01	784.9						
35.00	804.5	35.00	773.2	40.00	768.2	60.01	831.5	65.00	828.3	65.00	805.9						
40.00	828.0	40.00	797.6	45.01	792.2	65.00	851.9										
45.01	850.2	45.01	821.0	50.00	814.8												
50.00	871.4	50.00	842.8	55.00	836.4												
55.00	891.7	55.00	863.6	60.00	857.0												
60.01	910.9	60.00	883.6	65.00	876.6												
65.00	929.5	65.00	902.7														

tively. CO_2 was supplied by Air Liquide and had a purity greater than 99.99 %. The mixtures were prepared in small stainless steel cylinders, and the compositions were determined by weighing.

Sound-Speed Measurements. The speed of sound of liquid R404A was measured using an apparatus designed for high pressures, with an acoustic cell placed inside a stainless steel container, using a pulse-echo method at a frequency of 1 MHz as previously described.[6−9] The cell calibration was performed by measuring the speed of sound of pure CCl_4 at 10 MPa and 298.15 K and comparing the obtained value with data reported in the literature.[18,19] To cover the complete experimental temperature and pressure ranges, the calibration was expanded by the use of the thermal and pressure behavior of the pure copper spacers (purity better than 99.99 %). The steel container and the acoustic cell were thermostated inside a Dewar vessel within the temperature range from T = 258 K to T = 338 K, with a control system based on a two-stage cascaded thermostatic baths. The long-term stability of the complete system was within ± 0.02 K in the whole range, and the temperature measurements were taken with a four-wire platinum resistance thermometer previously calibrated to an uncertainty of ± 0.01 K on the ITS 90 scale. Pressure measurements were performed in two separate ranges with Setra Systems Inc. pressure transducers, one from vapor pressure to 35 MPa and the other up to 65 MPa. The pressure sensors were calibrated against a dead weight gauge with an uncertainty of ± 0.025 MPa in the lower range and ± 0.076 MPa in the higher range.

Taken into account all the error sources, the accuracy of the speed of sound measurements is estimated to be better than ± 0.1 m·s^{-1}. Several measurements were repeated at the same pressure and temperature conditions, allowing us to estimate a precision of ± 0.3 m·s^{-1}.

Measurements of Critical Data. The experimental apparatus for the critical data acquisition has already been described in detail[14,15] and was used unmodified in this study.

The acoustic cell is constructed from a stainless steel 3/8 in. cross piece, with its inner diameter bored out to provide an acoustic cavity of about 5 mL volume. Pressure was generated via a hand pump (High-Pressure Equipment Co., model 62-6-10) and monitored with a pressure transducer (Omega, model PX931) with a precision of ± 0.01 MPa. Temperature was measured on the ITS-90 with a precision of ± 0.001 K with a calibrated platinum resistance thermometer (Tinsley) connected to a digital multimeter (Keithley, model 2000). A pulse generator (Wavetek, Model 80) provided the acoustic signal, with a frequency of about 300 kHz. The signal was fed into the acoustic cavity via a piezoelectric ceramic transducer disk (Morgan Matroc Ltd., PC4D) with a thickness of 2 mm and a diameter of 6 mm. A second, identical transducer monitored the signal at the other end of the cavity. The transit times of the pulse across the acoustic cavity were displayed in an oscilloscope

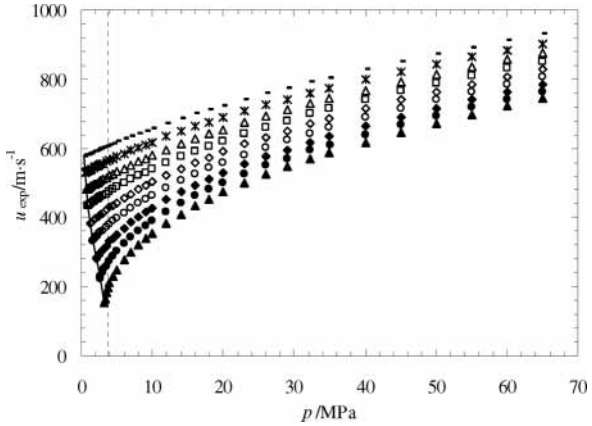

Figure 1. Experimental speed of sound, u, for R404A as a function of pressure at −, 258.13 K; *, 268.12 K; △, 278.11 K; □, 288.18 K; ◇, 298.17 K; ○, 308.17 K; ◆, 318.16 K; ●, 328.18 K; ▲, 338.19 K; —, saturation line; ---, critical pressure.

Table 2. Orthobaric Speed of Sound Data for R404A

T	Ps	u_σ	T	Ps	u_σ	T	Ps	u_σ
K	MPa	m·s^{-1}	K	MPa	m·s^{-1}	K	MPa	m·s^{-1}
258.13	0.37	577.1[a]	288.18	0.95	433.0	318.16	2.06	279.3
268.12	0.52	529.6	298.17	1.26	383.9	328.18	2.59	221.3
278.11	0.71	481.9	308.17	1.62	332.9	338.19	3.22	155.1

[a] Indicates extrapolated value.

Table 3. Coefficients of Equation 2 for the Orthobaric Speed of Sound u_σ

i	a_i	i	a_i
0	1.057202E+02	3	−2.147078E+04
1	−2.634315E+03	4	−2.531193E+04
2	−7.577463E+03		

Table 4. Coefficients of Equation 3 for the Speed of Sound of R404A Valid from T = 258 K to 328 K and Pressures from Saturation up to 65 MPa

a_{ij}	j		
i	0	1	2
0	1.723744E+03	−9.549537E+00	1.308442E−02
1	−6.414516E+01	4.878620E−01	−8.440610E−04
2	3.558126E−01	−4.392709E−03	1.196711E−05
b_{kl}	l		
k	0	1	2
0	1	−3.048597E−03	2.196759E−07
1	−5.047944E−02	2.956216E−04	−3.013833E−07
2	6.982797E−04	−6.410766E−06	1.440716E−08

(Tektronix, model TDS-340). The acoustic cell was immersed in a 40 L water bath, thermostated with a refrigeration unit and a temperature controller from Hart Scientific, with a RTD probe. This unit provides a temperature control within ± 0.004 K.

A mixture with a desired composition was obtained by weighing and was pumped into the acoustic cell. The pressure was increased with the hand pump until only minute changes in the acoustic signal were observed, meaning that a liquid-like state with a low compressibility was present in the acoustic cell. The system was allowed to equilibrate for at least 30 min at the desired starting temperature. Experiments were carried out at constant temperature, and pressure was lowered until a maximum in time delay was observed. Temperature was then systematically varied, and the procedure was repeated. The temperature and pressure values corresponding to the absolute maximum of time delay in the ensemble of the isothermal curves

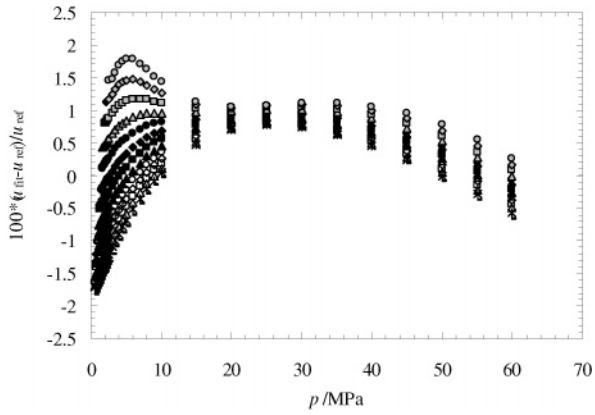

Figure 2. Percentage deviations $\{100\cdot(u_{fit} - u_{ref}/u_{ref}\}$ of the calculated speed of sound, u_{fit}, to refprop data, u_{ref}. of R404A: −, 260 K; *, 265 K; △, 270 K; □, 275 K; ◇, 280 K; ○, 285K; ▲, 290 K; ◆, 300 K; ●, 305 K; ▲, 310 K; ■, 315 K; ◆, 320 K; ●, 325 K.

(t_{delay}/μs vs p/MPa) were taken as the critical temperature and critical pressure.

Results

Speed of Sound of Liquid R404A. The apparatus was used to take a total of 328 experimental speed of sound measurements of the alternative refrigerant mixture R404A, within the referred temperature and pressure ranges. These data are shown in Table 1. The measurements were performed and organized as isotherms, within a total of 9, and are plotted in Figure 1. Fitting each one with tested the consistency of the individual isotherms:

$$u = \sum_{i=0}^{2} A_i \cdot [\ln(p - B_i)]^i \tag{1}$$

The standard deviations of the fits are smaller than 0.12 m·s^{-1} for isotherms in which the reduced temperature is lower than 0.90. For the isotherms at 318 K, 328 K, and 338 K, which correspond to reduced temperatures of 0.92, 0.95, and 0.98, the standard deviations of the fits are 0.20 m·s^{-1}, 0.28 m·s^{-1}, and 0.88 m·s^{-1}, respectively. This increase in the standard deviation of the fits can be explained by the proximity of the critical temperature and consequently abrupt changes in the speed of sound measures when we are close to the critical point, as can be seen in Figure 1.

It was possible to measure the saturated liquid (orthobaric) speed of sound, u_σ, for all isotherms except 258 K, where eq 1 was used to extrapolate the speed of sound at this temperature to the vapor pressure (REFPROP). The orthobaric speed of sound data presented in Table 2 were fitted to

$$u_\sigma = \sum_{i=0}^{4} a_i \cdot \left[\ln\left(\frac{T}{T_c}\right)\right]^i \tag{2}$$

(critical data T_c = 344.97 K) with the coefficients of Table 3. The standard deviation of the fit was 0.34 m·s^{-1}.

Finally, the set of experimental data excluding the isotherm at 338 K was fitted to

$$u = \frac{\sum_{i=0}^{2}\sum_{j=0}^{2} a_{ij} p^i T^j}{\sum_{k=0}^{2}\sum_{l=0}^{2} b_{kl} p^k T^l} \tag{3}$$

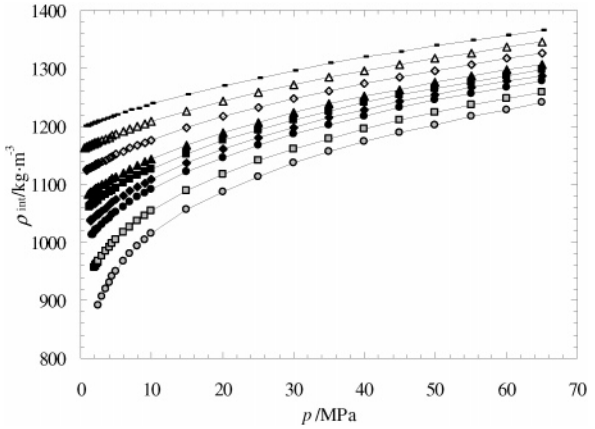

Figure 3. Density data of R404A, calculated through the integration procedure, as a function of pressure: −, 260 K; △, 270 K; ◇, 280 K; ▲, 290 K; ◆, 300 K; ●, 305 K; ■, 315 K; ◆, 320 K; ●, 325 K.

Table 5. Coefficients Used to Fit the Literature Density d_i and Heat Capacity Data c_j with Equations 14 and 15, Respectively

i	d_i	c_j
0	4.679446E+04	−4.132722E+05
1	−8.073604E+02	7.384030E+03
2	5.776228E+00	−5.262981E+01
3	−2.075036E−02	1.875951E−01
4	3.733711E−05	−3.344353E−04
5	−2.697304E−08	2.387072E−07

with the coefficients shown in Table 4 and a standard deviation of 0.37 $m \cdot s^{-1}$. The comparison between our fitted speed of sound data and the results obtained from REFPROP are presented in Figure 2. The deviations are slightly high, but this can be related with the mixing rule or with the functional form used in the commercial package. As far as we are aware of, there are no other speed of sound experimental data to which the present work can be compared.

Derived Thermodynamic Properties. The speed of sound, u, is directly related to the pressure derivative of the density, ρ, through eq 4 in which the subscript S denotes the condition of constant entropy:

$$\left(\frac{\partial \rho}{\partial p}\right)_S = \frac{1}{u^2} \tag{4}$$

This derivative is related to the isothermal pressure derivative and the isobaric temperature derivative of the density through eq 5, where C_P is the specific heat capacity at constant pressure:

$$\left(\frac{\partial \rho}{\partial p}\right)_S = \left(\frac{\partial \rho}{\partial p}\right)_T - \frac{T}{\rho^2 \cdot C_P}\left(\frac{\partial \rho}{\partial T}\right)_p^2 \tag{5}$$

Rearranging the last equation and combining it with eq 4, follows eq 6, which also incorporates the definition of the thermal expansion coefficient, α_p:

$$\left(\frac{\partial \rho}{\partial p}\right)_T = \frac{1}{u^2} + \frac{T}{C_P}\cdot\alpha_p^2 \tag{6}$$

$$\alpha_p = -\frac{1}{\rho}\left(\frac{\partial \rho}{\partial T}\right)_p \tag{7}$$

It can also be shown that the pressure partial derivative of the isobaric heat capacity can be calculated with eq 8:

$$\left(\frac{\partial C_P}{\partial p}\right)_T = -\frac{T}{\rho}\cdot\left[\alpha_p^2 + \left(\frac{\partial \alpha_p}{\partial T}\right)_p\right] \tag{8}$$

This way, given an isobar of the density and of C_P, it is possible to integrate eqs 6 and 8 over the pressure, thus obtaining the (p, ρ, T) and (p, C_P, T) surfaces within the range of pressure and temperature of the experimental speed of sound data. The numerical integration procedure also allows, through the use of eqs 9 to 13, the calculation of other properties, such as the isentropic compressibility, κ_S; the isothermal compressibility κ_T; the isochoric heat capacity, C_V; the thermal pressure coefficient, γ_V; and the isenthalpic Joule−Thomson coefficient, μ_{JT}:

$$\kappa_S = \frac{1}{\rho \times u^2} \tag{9}$$

$$\kappa_T = \frac{1}{\rho}\left(\frac{\partial \rho}{\partial p}\right)_T \tag{10}$$

$$C_V = C_P\frac{\kappa_S}{\kappa_T} \tag{11}$$

$$\gamma_V = \frac{\alpha_p}{\kappa_T} \tag{12}$$

$$\mu_{JT} = \frac{T\cdot\alpha_p - 1}{\rho\cdot C_P} \tag{13}$$

In the present work, due to the scarcity of experimental density available, to the best of our knowledge no isobaric heat capacity data exist in the literature, the authors used data from the commercial available program REFPROP at a pressure of 5 MPa and temperature from 250 K to 330 K. These isobars were fitted

Table 6. Calculated Densities ρ for R404A as a Function of Temperature T and Pressure p

	ρ/(kg·m^{-3})								
p/MPa	T = 260 K	T = 270 K	T = 280 K	T = 290 K	T = 295 K	T = 300 K	T = 305 K	T = 315 K	T = 325 K
1.0	1201.8	1165.4	1125.8						
2.5	1208.7	1173.6	1136.0	1095.1	1073.0	1049.7	1024.6	967.0	892.3
5.0	1219.4	1186.2	1151.1	1113.7	1093.9	1073.3	1051.6	1004.6	950.4
10.0	1238.4	1208.1	1176.7	1143.9	1126.9	1109.5	1091.6	1054.2	1014.3
15.0	1255.1	1226.9	1198.1	1168.3	1153.1	1137.6	1121.9	1089.5	1056.0
20.0	1270.0	1243.5	1216.6	1189.1	1175.1	1160.9	1146.6	1117.5	1087.8
25.0	1283.6	1258.4	1233.0	1207.2	1194.2	1181.0	1167.8	1141.0	1113.9
30.0	1296.1	1272.0	1247.8	1223.4	1211.1	1198.8	1186.3	1161.3	1136.1
35.0	1307.8	1284.5	1261.4	1238.1	1226.4	1214.7	1202.9	1179.3	1155.5
40.0	1318.7	1296.1	1273.9	1251.6	1240.4	1229.2	1218.0	1195.5	1173.0
45.0	1328.9	1307.0	1285.5	1264.0	1253.3	1242.6	1231.8	1210.3	1188.7
50.0	1338.6	1317.2	1296.4	1275.7	1265.3	1255.0	1244.6	1223.9	1203.2
55.0	1347.8	1326.9	1306.6	1286.5	1276.5	1266.5	1256.6	1236.5	1216.6
60.0	1356.7	1336.1	1316.3	1296.8	1287.1	1277.4	1267.8	1248.4	1229.1
65.0	1365.1	1344.9	1325.5	1306.5	1297.1	1287.7	1278.3	1259.5	1240.9

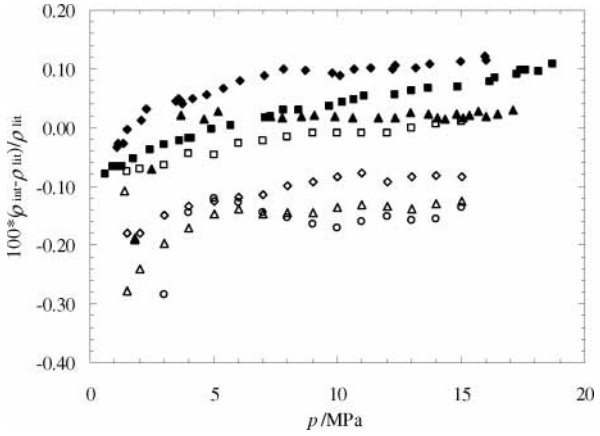

Figure 4. Plot of deviations between our results and the literature experimental densities. Bouchot and Richon:[20] ■, 273.19 K; ◆, 293.18 K; ▲, 313.2 K. Fujiwara et al.:[2,3] □, 263.15 K; ◇, 283.15 K; △, 303.15 K; ○, 323.15 K.

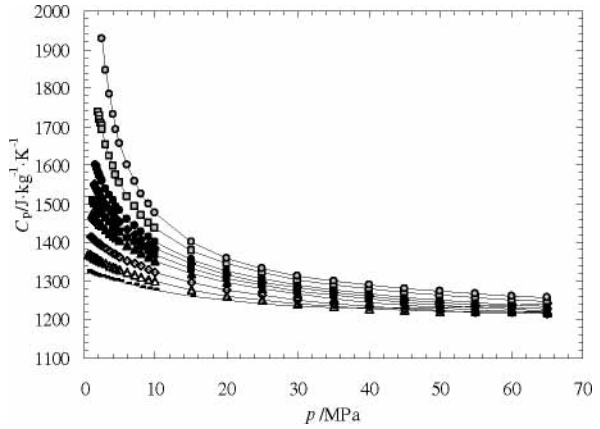

Figure 5. Isobaric heat capacity, C_P, of R404A calculated through the integration procedure: −, 260 K; △, 270 K; ◇, 280 K; ▲, 290 K; ■, 295 K; ◆, 300 K; ●, 305 K; ■, 315 K; ●, 325 K.

to eqs 14 and 15 with the coefficients of Table 5:

$$\rho(T, 5\ \text{MPa}) = \sum_{i=0}^{5} d_i \cdot T^i \qquad (14)$$

$$C_P(T, 5\text{MPa}) = \sum_{j=0}^{5} c_j \cdot T^j \qquad (15)$$

The integration procedure was implemented both on increasing pressure, up to 65 MPa, and on decreasing pressure, down to the saturation line.

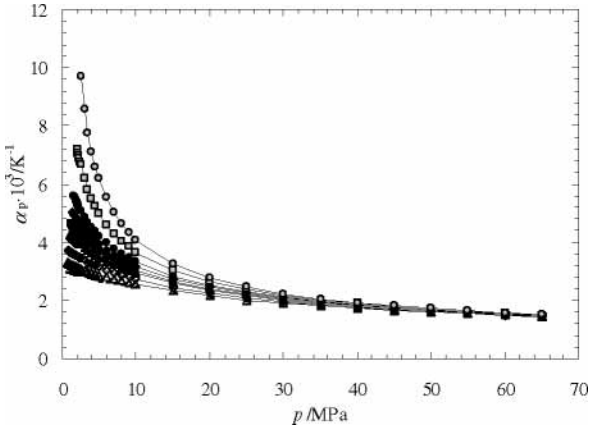

Figure 6. Thermal expansion coefficient, α_p, of R404A calculated through the integration procedure: −, 260 K; △, 270 K; ◇, 280 K; ▲, 290 K; ■, 295 K; ◆, 300 K; ●, 305 K; ■, 315 K; ●, 325 K.

The whole (p, ρ, T) surface obtained using the integration procedure, previously described is shown in Figure 3 and Table 6. To test the results, the whole set of calculated density data were fitted with an equation similar to eq 3, with a standard deviation of 0.06 %. Figure 4 represents the percentage deviation between the fitted density results and the available experimental densities taken from two different authors.[2,3,20] As it can be seen, our results are in good agreement with the experimental densities as long as they fall precisely in the middle of both reported measurements. The complete (p, C_P, T) surface is plotted in Figure 5 and Table 7. The other thermodynamic properties calculated are represented in Figures 6 through 8 and in Tables 8 to 10.

Critical Behavior. Our acoustic method was applied to investigate the critical properties of R404A and CO_2 + R404A system. The refrigerant used in this study is a near azeotropic mixture, which means that its behavior is similar to that one of a pure component. We considered R404A as a pure component and treated the mixture with CO_2 as a binary mixture and not ternary or quaternary mixtures. The estimated errors of the critical parameters reported are ± 0.1 K for the critical temperature and 0.05 MPa for the critical pressure. The estimate was based on a comparison of the results of different experiments performed with the same mixture and is mainly determined by the narrowness of the isotherms studied as during an experiment the pressure decreases in a continuous way.

R404A. The acoustic experiments are carried out at constant temperature and the pressure is lowered until a maximum in time delay is observed, meaning that it has reached a local maximum in the compressibility, corresponding to a phase

Table 7. Calculated Isobaric Heat Capacity C_P for R404A as a Function of Temperature T and Pressure p

	C_P/(J·kg^{-1}·K^{-1})								
p/MPa	T = 260 K	T = 270 K	T = 280 K	T = 290 K	T = 295 K	T = 300 K	T = 305 K	T = 315 K	T = 325 K
1.0	1321	1365	1413						
2.5	1311	1349	1391	1443	1475	1512	1559	1692	1927
5.0	1299	1329	1363	1404	1427	1453	1482	1553	1656
10.0	1277	1298	1324	1353	1368	1384	1401	1435	1475
15.0	1261	1277	1297	1320	1332	1344	1356	1379	1400
20.0	1249	1261	1278	1297	1307	1317	1327	1344	1358
25.0	1241	1249	1263	1280	1289	1298	1306	1321	1332
30.0	1235	1240	1251	1266	1274	1282	1290	1304	1313
35.0	1232	1233	1241	1255	1262	1270	1278	1291	1299
40.0	1230	1228	1234	1245	1253	1260	1267	1280	1289
45.0	1230	1225	1228	1238	1244	1251	1258	1271	1280
50.0	1231	1223	1223	1231	1237	1244	1251	1264	1273
55.0	1233	1221	1219	1226	1231	1237	1244	1257	1267
60.0	1237	1222	1217	1221	1226	1232	1238	1251	1261
65.0	1242	1223	1215	1217	1222	1227	1233	1246	1256

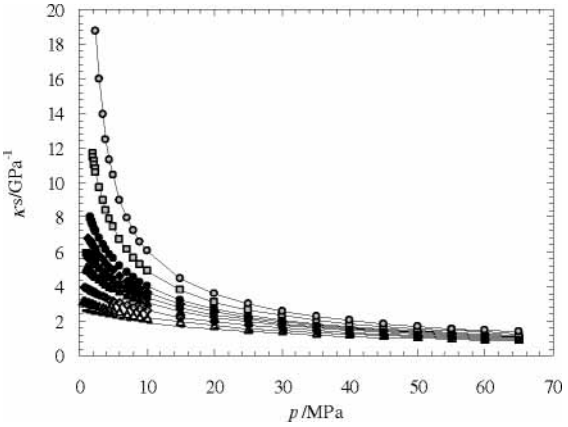

Figure 7. Isentropic compressibility, κ_S, of R404A calculated through the integration procedure: −, 260 K; △, 270 K; ◇, 280 K; ▲, 290 K; ■, 295 K; ◆, 300 K; ●, 305 K; ■, 315 K; ●, 325 K.

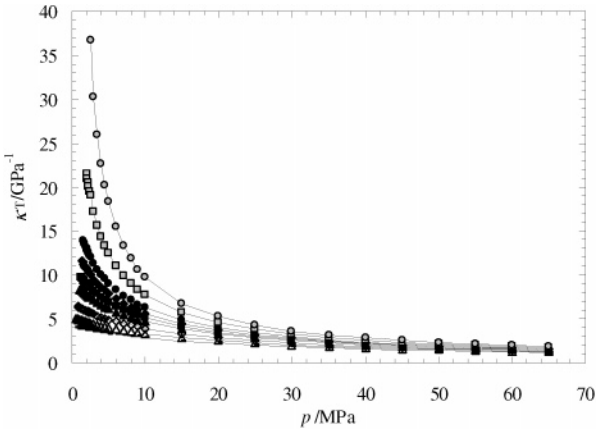

Figure 8. Isothermal compressibility, κ_T, of R404A calculated through the integration procedure: −, 260 K; △, 270 K; ◇, 280 K; ▲, 290 K; ■, 295 K; ◆, 300 K; ●, 305 K; ■, 315 K; ●, 325 K.

transition. The temperature is then systematically varied and the procedure repeated. Several isotherms were measured in the vicinity of the critical temperature. The temperature and pressure values corresponding to the absolute maximum of time delay in the ensemble of the isothermal curves is taken as the critical temperature and pressure.

The critical properties for R404A have recently been investigated by Fujiwara et al.[2,3] and by Bouchot and Richon[20] using visual methods. Fujiwara et al. reported a critical temperature of 345.15 K and a critical pressure of 3.726 MPa, while Bouchot and Richon reported only the critical temperature of 344.7 K. The critical properties obtained by our acoustic method are 344.97 K for critical temperature and 3.733 MPa for critical pressure. As it can be concluded the acoustic results measured in our apparatus are in agreement with the literature values within the combined experimental errors.

CO_2 + R404A. The critical line of CO_2 + R404A mixture was determined over the whole composition range. Acoustic measurements were performed on seven mixtures. The experimental critical parameters, T_c and p_c, are shown in Table 11 for each mixture and are plotted in Figure 9. The system exhibits type I fluid phase behavior, according to the classification of van Konynenburg and Scott, which means that a continuous critical line connects the critical points of R404A and CO_2. This system behaves almost ideally. The projections of critical line are almost straight lines connecting the critical points. No

Table 8. Calculated Isobaric Thermal Expansion Coefficient α_p for R404A as a Function of Temperature *T* and Pressure *p*

	α_p/K^{-1}								
p/MPa	*T* = 260 K	*T* = 270 K	*T* = 280 K	*T* = 290 K	*T* = 295 K	*T* = 300 K	*T* = 305 K	*T* = 315 K	*T* = 325 K
1.0	2.920	3.248	3.675						
2.5	2.864	3.078	3.447	3.922	4.221	4.594	5.083	6.658	9.725
5.0	2.664	2.870	3.143	3.485	3.692	3.933	4.219	4.990	6.179
10.0	2.410	2.551	2.726	2.934	3.052	3.180	3.322	3.655	4.084
15.0	2.224	2.321	2.444	2.585	2.663	2.744	2.831	3.021	3.243
20.0	2.080	2.147	2.235	2.339	2.394	2.451	2.509	2.632	2.765
25.0	1.965	2.008	2.074	2.152	2.193	2.236	2.278	2.364	2.452
30.0	1.870	1.896	1.944	2.004	2.036	2.069	2.102	2.166	2.228
35.0	1.792	1.802	1.836	1.883	1.909	1.935	1.962	2.011	2.056
40.0	1.726	1.723	1.745	1.782	1.803	1.825	1.846	1.886	1.921
45.0	1.671	1.656	1.668	1.696	1.713	1.731	1.749	1.782	1.810
50.0	1.624	1.598	1.601	1.621	1.635	1.650	1.665	1.694	1.717
55.0	1.584	1.547	1.542	1.556	1.567	1.579	1.592	1.617	1.636
60.0	1.551	1.503	1.490	1.497	1.506	1.516	1.527	1.549	1.566
65.0	1.522	1.465	1.443	1.445	1.451	1.460	1.469	1.488	1.504

Table 9. Calculated Isentropic Compressibility κ_S for R404A as a Function of Temperature *T* and Pressure *p*

	κ_S/GPa^{-1}								
p/MPa	*T* = 260 K	*T* = 270 K	*T* = 280 K	*T* = 290 K	*T* = 295 K	*T* = 300 K	*T* = 305 K	*T* = 315 K	*T* = 325 K
1.0	2.524	3.104	3.919						
2.5	2.390	2.900	3.594	4.580	5.242	6.072	7.141	10.582	18.786
5.0	2.199	2.622	3.174	3.910	4.377	4.930	5.597	7.424	10.407
10.0	1.907	2.219	2.602	3.078	3.361	3.679	4.040	4.919	6.081
15.0	1.693	1.937	2.225	2.570	2.767	2.984	3.222	3.776	4.456
20.0	1.529	1.727	1.955	2.221	2.369	2.530	2.703	3.095	3.557
25.0	1.398	1.563	1.751	1.963	2.081	2.206	2.340	2.636	2.975
30.0	1.290	1.431	1.589	1.765	1.861	1.962	2.069	2.303	2.565
35.0	1.200	1.322	1.457	1.606	1.686	1.771	1.859	2.050	2.261
40.0	1.123	1.230	1.348	1.476	1.545	1.617	1.692	1.851	2.025
45.0	1.056	1.151	1.255	1.368	1.427	1.490	1.554	1.691	1.838
50.0	0.997	1.083	1.175	1.276	1.328	1.383	1.440	1.559	1.686
55.0	0.945	1.022	1.106	1.196	1.244	1.293	1.343	1.449	1.560
60.0	0.898	0.969	1.046	1.127	1.170	1.215	1.260	1.355	1.455
65.0	0.856	0.922	0.992	1.067	1.106	1.147	1.188	1.274	1.364

Table 10. Calculated Isothermal Compressibility κ_T for R404A as a Function of Temperature T and Pressure p

	κ_T/GPa^{-1}								
p/MPa	T = 260 K	T = 270 K	T = 280 K	T = 290 K	T = 295 K	T = 300 K	T = 305 K	T = 315 K	T = 325 K
1.0	3.921	4.895	6.296						
2.5	3.735	4.515	5.699	7.402	8.563	10.060	12.076	19.115	36.657
5.0	3.363	4.034	4.936	6.163	6.952	7.906	9.081	12.450	18.291
10.0	2.862	3.339	3.937	4.691	5.142	5.655	6.241	7.701	9.704
15.0	2.506	2.865	3.301	3.826	4.128	4.461	4.829	5.690	6.768
20.0	2.238	2.520	2.856	3.249	3.470	3.708	3.966	4.548	5.239
25.0	2.028	2.256	2.524	2.833	3.003	3.184	3.378	3.804	4.292
30.0	1.858	2.046	2.266	2.517	2.653	2.797	2.949	3.279	3.646
35.0	1.718	1.876	2.060	2.268	2.381	2.499	2.623	2.887	3.176
40.0	1.600	1.734	1.890	2.067	2.162	2.262	2.365	2.584	2.819
45.0	1.500	1.614	1.748	1.901	1.983	2.068	2.156	2.341	2.538
50.0	1.413	1.511	1.628	1.761	1.832	1.906	1.983	2.143	2.312
55.0	1.338	1.421	1.524	1.641	1.704	1.770	1.837	1.978	2.125
60.0	1.271	1.343	1.434	1.538	1.594	1.653	1.713	1.839	1.969
65.0	1.212	1.274	1.354	1.448	1.499	1.551	1.606	1.719	1.836

Table 11. Experimental Critical Data, p_c and T_c, of the System CO_2 + R404A

xCO$_2$	p_c/MPa	T_c/K	xCO$_2$	p_c/MPa	T_c/K
0.979	7.29	305.6	0.748	6.44	319.5
0.959	7.15	307.3	0.496	5.57	328.8
0.920	7.03	309.2	0.152	4.46	338.51
0.816	6.57	315.3	0.000	3.73	344.97

maxima or minima in the projections of the critical line are visible. This suggests that R404A should be a useful modifier for CO_2. Its relatively low critical temperature (344.97 K) and its miscibility with CO_2 make it potentially attractive as modifier for improving solubility in supercritical CO_2. As can be seen from Figure 9, the critical pressure of the system goes from p_C of pure CO_2, down to 3.733 MPa, the critical pressure of R404A. This means that as R404A is added to CO_2 the solvation properties of the mixture will have substantially changed but the critical temperature and critical pressure remain reasonably low. As a result R404A could conveniently be used to modify CO_2.

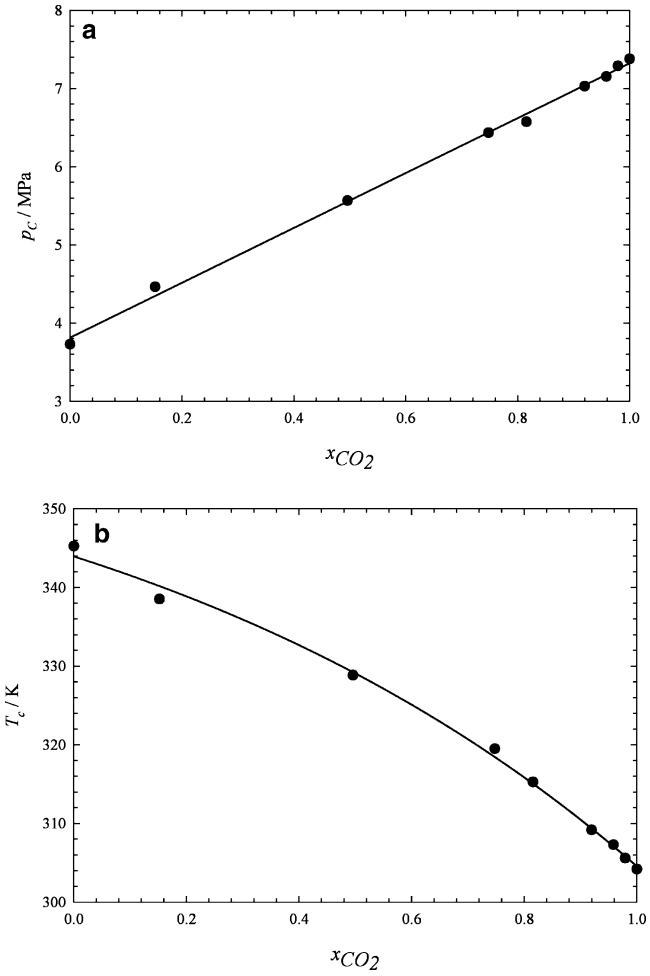

Figure 9. Projections of the critical curve for the xCO$_2$ + (1 − x)R404A system: a, $p-x$ projection; b, $T-x$ projection.

Table 12. Parameters of the Pure Substances Used in the Peng−Robinson Equation of State

component	p_c/MPa	T_c/K	ω_i
CO_2	7.38[25,26]	304.13[26]	0.239[27]
R404A	3.73[28]	344.97	0.278

Correlation of Results and Discussion. Experimental critical data were correlated with the Peng−Robinson equation of state (PR EOS)[21] that is a cubic EOS based on a one-fluid model:

$$p = \frac{RT}{(V_m - b)} - \frac{a(T)}{V_m(V_m + b) + b(V_m - b)} \tag{16}$$

In its extension to binary mixtures, the characteristic parameters a and b are calculated using the following van der Waals one-fluid mixing rules, which assume random distribution of molecules:

$$a = x_1^2 a_1 + 2x_1x_2a_{12} + x_2^2 a_2 \tag{17}$$

$$b = x_1^2 b_1 + 2x_1x_2b_{12} + x_2^2 b_2 \tag{18}$$

In these equations x_i is the mole fraction of component i (i = 1, 2), and a_i and b_i are pure component parameters defined by Peng and Robinson.[21] In particular, $a_i(T) = a_{c,i}(T_{c,i})$ $\alpha_i(T,\beta_i(\omega_i))$, where ω_i is Pitzer's acentric factor of molecule i. The combining rules for the binary cross-interaction parameters a_{12} and b_{12} are given by:

$$a_{12} = (a_1a_2)^{1/2}(1 - k_{12}) \tag{19}$$

$$b_{12} = \frac{1}{2}(b_1 + b_2)(1 - l_{12}) \tag{20}$$

Here k_{12} and l_{12} and parameters describing deviations from, respectively, the geometric and arithmetic mean combining rules. Values of critical temperature, critical pressure, and acentric factor[22,23] for each pure fluid which are presented in Table 12, constitute, along with the deviation parameters, the model input variables for PR EOS. R404A acentric factor was calculated using the definition of Pitzer[24] and the experimental data T_c/P_c and vapor pressures reported by Solvay Technical Data Sheets.[28]

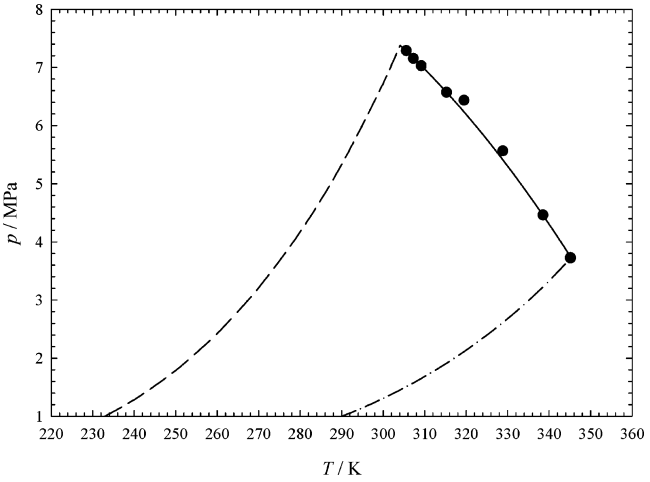

Figure 10. $p-T$ projection of the critical line for the $x\mathrm{CO_2} + (1 - x)$-R404A system: ●, acoustic data; −, predicted critical line with PR-EOS; ---, vapor pressure curves for $\mathrm{CO_2}$;[27] $-\cdot-$, vapor pressure curve for R404A.[28]

The deviation parameters, k_{12} and l_{12} were varied so that the theoretical critical line would give the best fit of the experimental data for each binary system. Although the deviation parameters are often fitted to the experimental critical data using only the equimolar mixture,[16] we used all the experimental data available for evaluating these parameters. The deviation parameters of $\mathrm{CO_2}$ + R404A that gave the best fit were $k_{12} = 0.00015$ and $l_{12} = 0.02$. Figure 10 shows the (p, T) projection of the critical line for this system using the optimized interaction parameters and the pure component vapor pressures for the binary system. It can be seen from this figure that the PR EOS gives a reasonable agreement with the experimental data for this binary system.

Conclusions

The thermophysical properties and critical parameters for the alternative refrigerant R404A (52 wt % of 1,1,1-trifluoroethane (R143a) + 44 wt % of pentafluoroethane (R125) + 4 wt % of 1,1,1,2-tetrafluoroethane (R134a)) were investigated using two different acoustic techniques. The critical behavior of the system $x\mathrm{CO_2} + (1 - x)$R404A was also investigated over the whole composition range. With mole fractions of up to 10 % of R404A, critical temperature only increases 4 K, and the critical pressure decreases 0.3 MPa. The critical line show type I fluid phase behavior. The results were well correlated with the PR EOS using conventional mixing and combining rules.

Literature Cited

(1) Li, J.; Tillner-Roth, R.; Sato, H.; Watanabe, K. Equation of state for hydrofluorocarbon refrigerant mixtures of HFC-125/143a, HFC-125/134a, HFC-134a/143a and HFC-125/134a/143a. *Fluid Phase Equilib.* **1999**, *161*, 225−239.

(2) Fujiwara, K.; Nakamura, S.; Noguchi, M. Thermodynamic properties for R-404A. *Int. J. Thermophys.* **1999**, *20*, 129−140.

(3) Fujiwara, K.; Nakamura, S.; Noguchi, M. Critical parameters and *PVT* properties for R-404A. *J. Chem. Eng. Data* **1998**, *43*, 967−972.

(4) Jannick, P.; Meurer, C. Replacement of R22 and future trends in refrigeration and air conditioning. *Solvay Fluor und Derivate GmbH 10th International Conference*, Jaszbereny, Hungary, 2000; pp 1−9.

(5) Solkane 404A Thermodynamics−Solvay Fluor und Derivate GmbH, Technical Service, Refrigerants Product Bulletin T/10.00/02/E, 2000.

(6) Pires, P. F.; Guedes, H. J. R. The speed of sound and isentropic compressibility of liquid difluoromethane (HFC32) from $T =$ (248 to 343) K and pressures up to 65 MPa *J. Chem. Thermodyn.* **1999**, *31*, 55−69.

(7) Pires, P. F.; Guedes, H. J. R. The speed of sound, and derived thermodynamic properties of liquid trifluoromethane (HFC23) from $T =$ (258 to 303) K at pressures up to 65 MPa *J. Chem. Thermodyn.* **1999**, *31*, 479−490.

(8) Pires, P. F.; Esperança, J. M. S. S.; Guedes, H. J. R. Ultrasonic speed of sound and derived thermodynamic properties of liquid 1,1,1,2,3,3,3-heptafluoropropane (HFC227ea) from 248 K to 333 K and pressures up to 65 MPa. *J. Chem. Eng. Data* **2000**, *45*, 496−501.

(9) Gomes de Azevedo, R.; Szydlowski, J.; Pires, P. F.; Esperança, J. M. S. S.; Guedes, H. J. R.; Rebelo, L. P. N. A novel non-intrusive microcell for sound-speed measurements in liquids. Speed of sound and thermodynamic properties of 2-propanone at pressures up to 160 MPa. *J. Chem. Thermodyn.* **2004**, *36*, 211−222.

(10) McLinden, M. O.; Klein, S. A.; Lemmon, E. W.; Peskin, A. P. *REFPROP*, NIST Standard Reference Database 23. Version 6.01; Standard Reference Data Program: Gaithersburg, MD, 1998.

(11) Sun, T.; Biswas, S. N.; Trappeniers, N. J.; Seldam, C. A. T. Acoustic and thermodynamic properties of methanol from 273 to 333 K and at pressures to 280 MPa. *J. Chem. Eng. Data* **1988**, *33*, 395−398.

(12) Kordikowski, A.; Robertson, D. G.; Aguiar-Ricardo, A.; Popov, V. K.; Howdle, S. M.; Poliakoff, M. Probing vapor/liquid equilibria of near-critical binary gas mixtures by acoustic measurements *J. Phys. Chem.* **1996**, *100*, 9522.

(13) Kordikowski, A.; Robertson, D. G.; Poliakoff, M.; DiNoia, T. D.; McHugh, M.; Aguiar-Ricardo, A. Acoustic determination of the critical surfaces in the ternary systems $\mathrm{CO_2} + \mathrm{CH_2F_2} + \mathrm{CF_3CH_2F}$ and $\mathrm{CO_2} + \mathrm{C_2H_4} + \mathrm{CH_3CHCH_2}$ and in their binary subsystems. *J. Phys. Chem. B* **1997**, *101*, 5853.

(14) Ribeiro, N.; Casimiro, T.; Duarte, C.; Poliakoff, M.; Nunes da Ponte, M.; Aguiar-Ricardo, A. Vapor−liquid equilibrium and critical line of the $\mathrm{CO_2}$ + Xe system. Critical behavior of the $\mathrm{CO_2}$ + Xe versus $\mathrm{CO_2}$ + *n*-alkanes. *J. Phys. Chem. B* **2000**, *104*, 791−795.

(15) Ribeiro, N.; Aguiar-Ricardo, A. A simple acoustic probe for fluid phase equilibria: application to the $\mathrm{CO_2} + \mathrm{N(C_2H_5)_3}$ system. *Fluid Phase Equilib.* **2001**, *185*, 295−303.

(16) Ribeiro, N.; Aguiar-Ricardo, A.; Kordikowski, A.; Poliakoff, M. Acoustic determination of the critical surface of $\{x_1\mathrm{CO_2} + x_2\mathrm{C_2H_6} + (1 - x_1 - x_2)\mathrm{CHF_3}\}$. *Phys. Chem. Chem. Phys.* **2001**, *3*, 1027−1033.

(17) Reis, J. C. R.; Ribeiro, N.; Aguiar-Ricardo, A. Can the speed of sound be used for detecting critical states of fluid mixtures? *J. Phys. Chem. B* **2006**, *110*, 478−484.

(18) Kyohara, O.; Alpin, C. J.; Benson, G. C. Ultrasonic velocities, compressibilities, and heat capacities for binary mixtures of benzene, cyclohexane, and tetrachloromethane at 298.15 K. *J. Chem. Thermodyn.* **1978**, *10*, 721−730.

(19) Lainez, A.; Miller, J. F.; Zollweg, J. A.; Streett, W. B. Volumetric and speed-of-sound measurements for liquid tetrachloromethane under pressure. *J. Chem. Thermodyn.* **1987**, *19*, 1251−1260.

(20) Bouchot, C.; Richon, D.; P. V. T. VLE properties of several refrigerants (pure compounds and mixtures) through an original apparatus. *Proceedings of the 19th International Congress of Refrigeration*, The Hague, The Netherlands, Vol. IVA, 1995.

(21) Peng, D.; Robinson, D. A new two-constant equation of state. *Ind. Eng. Chem. Fundam.* **1976**, *15*, 59−64.

(22) Sandler, S. I.; Orbey, H.; Lee, B.-I. *Models for Thermodynamic and Phase Equilibria Calculations*; Sandler, S. I., Ed.; Marcel Dekker: New York, 1994; p 87.

(23) Prausnitz, J. M.; Lichtenthaler, R. N.; De Azevedo, E. G. *Molecular Theory of Fluid-Phase Equilibria*, 3rd ed.; Prentice Hall: Upper Saddle River, NJ, 1999; p 718.

(24) Pitzer, K. S. The volumetric and thermodynamic properties of fluids. I. Theoretical basis and virial coefficients. *J. Am. Chem. Soc.* **1955**, *77*, 3427−3433.

(25) Angus, S.; Armstrong, B. B.; de Reuck, K. M. *Carbon Dioxide−International Thermodynamic Tables of the Fluid State-3*; IUPAC, Pergamon Press: Oxford, U.K., 1976.

(26) Span, R.; Wagner, W. A new equation of state for carbon dioxide covering the fluid region from the triple-point temperature to 1100 K at pressures up to 800 MPa. *J. Phys. Chem. Ref. Data* **1996**, *25*, 1509−1596.

(27) Reid, R. C.; Prausnitz, J. M.; Pauling, B. E. *The Properties of Gases and Liquids*, 4th ed.; McGraw-Hill: New York, 1987.

(28) http://www.solvay.com, technical data sheets.

Received for review February 16, 2006. Accepted March 27, 2006. Financial support from Fundação para a Ciência e Tecnologia (FCT), FEDER, and FSE through Contracts PBIC/C/QUI/2134/95, POCTI/QUI/35429/2000, PraxisXXI/BD/16081/98, Praxis XXI/BD/19836/99, and Fundação Calouste Gulbenkian are gratefully acknowledged.

JE0600707